Bioinspired nervous signal transmission system based on two-dimensional laminar nanofluidics: From electronics to ionics

Yunfei Teng[a,b,1], Pei Liu[a,b,1], Lin Fu[a,b], Xiang-Yu Kong[a,2], Lei Jiang[a,b], and Liping Wen[a,b,2]

[a]CAS Key Laboratory of Bio-inspired Materials and Interfacial Science, Technical Institute of Physics and Chemistry, Chinese Academy of Sciences, 100190 Beijing, People's Republic of China; and [b]School of Future Technology, University of Chinese Academy of Sciences, 100049 Beijing, People's Republic of China

Edited by David A. Weitz, Harvard University, Cambridge, MA, and approved June 1, 2020 (received for review March 30, 2020)

Mammalian nervous systems, as natural ionic circuitries, stand out in environmental perception and sophisticated information transmission, relying on protein ionic channels and additional necessary structures. Prosperously emerged ionic regulated biomimetic nanochannels exhibit great potentialities in various application scenarios, especially signal transduction. Most reported direct current systems possess deficiencies in informational density and variability, which are superiorities of alternating current (AC) systems and necessities in bioinspired nervous signal transmission. Here, inspired by myelinated saltatory conduction, alternating electrostatic potential controlled nanofluidics are constructed with a noncontact application pattern and MXene nanosheets. Under time-variant external stimuli, ions confined in the interlaminar space obtain the capability of carriers for the AC ionic circuit. The transmitted information is accessible from typical sine to a frequency-modulated binary signal. This work demonstrates the potentiality of the bioinspired nervous signal transmission between electronics and ionic nanofluidics, which might push one step forward to the avenue of AC ionics.

biomimetic structures | nanofluidics | ion transportation | AC system | information transmission

The mammalian nervous system, as the most powerful natural ionic circuitry, demonstrates specific functions, such as multiple responsive abilities and high-throughput ionic information transmission. The natural system employs ions rather than electrons as its carriers (1), due to the aqueous nature of the organism. Within this aqueous ionic system, billions of stimulus–response combinations help the daily activities of living beings, and specific biological structures guarantee high efficiency (2, 3). These various fantastic capabilities have deeply interested researchers to pursue the fact and build an artificial ionic prototype (4) with simulated functions (5). In the natural nervous system, different physical and chemical stimuli would trigger corresponding responses by manipulating the magnitude of ionic current, and these functions are generally realized by various transfer proteins by simply changing their spatial configurations or the exposure of charged functional groups in the neural ionic circuitry. Once the ionic signal is generated, this ion-carried information would be sent across corresponding organs and tissues. Axons dedicated a lot to this procedure, which is one of the critical influencers in signal transmission procedure. This high-throughput ionic information transmission process relays on myelin sheaths, which seem to be neglected. Different from unmyelinated axons, myelinated axons employ a unique impulse propagation mechanism of saltatory conduction, in which the transmembrane ionic transportation would only appear at the node of Ranvier (6, 7), where the transmembrane ion transportation dominates (Fig. 1). In the past decades, a large number of distinctive stimuli were able to trigger corresponding designed responsive nanochannels with the dedication of electrical changeable functional groups (8) or molecular fragments (9) with controllable spatial configurations. However, to a great extent, it seems that applications of ionic current manipulation have been limited in research fields of the ionic diode (10) and its derivatives (11). To be noticed that, stimulus–response combinations in nervous systems are not only the avenue of perceiving the surrounding chemical environmental or thermodynamic variables but also the generator of all kinds of ionic information. It is promising to move one step forward to build artificial ionics systems for information transmission.

As to signal patterns, the wide application of direct current nanofluidics also reveals its weakness in informational description and transmission, whereas alternating current (AC) signal exhibits an innate potential in biomimetic informational transmission because of its more widely available patterns of waveforms and higher information density (12). Despite that some studies (13–16) have primarily introduced periodic environmental variables (17) to verify their devices' cycle stability or broad applicability, few of them have applied them for AC information transmission under time-variant external stimuli. In order to generate a stimuli-triggered alternating ionic current (AIC) signal, external field-driven directional ion transport is chosen as our method for ionic current manipulation. Among all kinds of stimulus–response combinations, external electrostatic potential

Significance

Mammalian nervous systems, as natural ionic circuitries, have interested researchers with their powerful abilities in environmental perceptions and information transmission, which triggered booming development in artificial prototypes such as biomimetic ionic nanochannels. Most studied artificial ionic systems are more focused on their functions of perception, whereas the ionic information transmission system is rarely reported. Here, two-dimensional laminar nanofluidics are fabricated from MXene nanosheets and the noncontact external electrostatic potential applied patterns to generate and transmit alternating signals, from basic sine to frequency-modulated binary information. This work demonstrates the potentiality of bioinspired nervous signal transmission to simulate the neural ion-carried information system, which might lead to the avenue of alternating current ionics.

Author contributions: Y.T., P.L., and X.-Y.K. designed research; Y.T. and P.L. performed research; Y.T., P.L., L.F., X.-Y.K., L.J., and L.W. analyzed data; Y.T., P.L., L.F., X.-Y.K., L.J., and L.W. wrote the paper; and L.W. guided the project.

The authors declare no competing interest.

This article is a PNAS Direct Submission.

[1]Y.T. and P.L. contributed equally to this work.

[2]To whom correspondence may be addressed. Email: wen@mail.ipc.ac.cn or kongxiangyu@mail.ipc.ac.cn.

This article contains supporting information online at https://www.pnas.org/lookup/suppl/doi:10.1073/pnas.2005937117/-/DCSupplemental.

First published July 1, 2020.

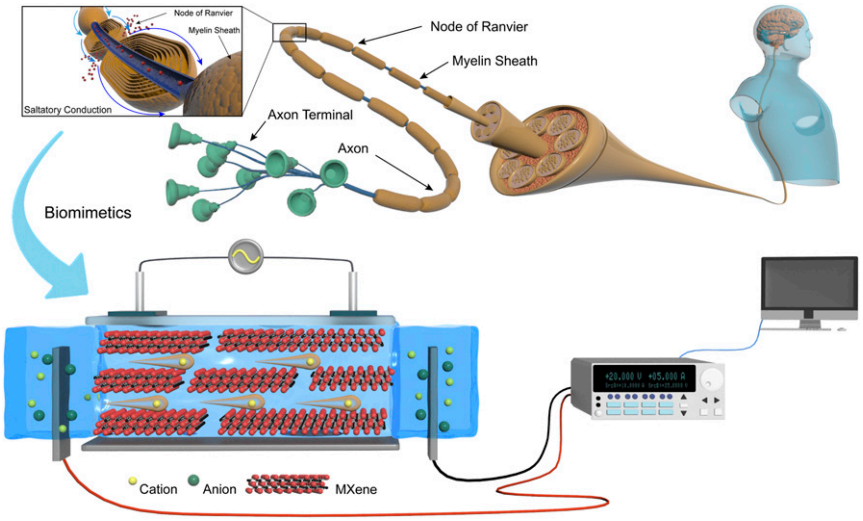

Fig. 1. The neural saltatory conduction along axons and bioinspired nervous signal transmission system. Saltatory conduction is a unique action potential propagation pattern, which is limited in myelinated axons and demonstrates an ultrafast signal transmission ability. The bioinspired nervous signal transmission system is a PDMS sealed 2D MXene nanofluidic device with additional signal input and acquisition modules. The signal image in the screen model is the real current feedback acquired by our nanofluidic devices. More detailed descriptions about our device can be seen in Fig. 2*A* and *SI Appendix*, Fig. S1.

belongs to the most fundamental and immediate species, which has been widely applied in fabricating field-effect transistor nanofluidics (18). Inspired by functions of myelin sheaths, the closure of nanofluidic would efficiently reduce unnecessary ion spread, especially for potential implantable and aqueous application scenarios. Proved by previous studies, it is believed that both inserted (19, 20) and noncontact (11, 21) methods are indispensable portions of nanofluidic fabrication approaches, whereas the noncontact pattern could guarantee the closure of nanofluidic and avoid the potentiality of the electrochemical reaction between units for applying stimuli and the carrier of nanofluidic devices. The noncontact pattern exhibits superiority in avoiding the undesired electrochemical reaction on inserted electrodes with the complete closure of their structures.

Here, an external electrostatic potential-driven ionic nanofluidic has been synthesized with the noncontact method for AC information transmission (Figs. 1 and 2*A*). For the sake of higher resolution in ionic signal transmission, polydimethylsiloxane (PDMS) sealed laminar MXene nanofluidics are taken as the ions' pathway, inspired by a myelin sheath. A pair of heavy p-doped silicon gates are applied for signal input. When the time-varying electrostatic potential is applied, it would directly influence the space density of carriers inside two-dimensional (2D) nanochannels. Thus, the controllable alternating ionic current is generated (Fig. 2*C*). To estimate the compatibility of transmitted information, sine signals with different amplitudes and frequencies are applied to the silicon chips. The current feedbacks exhibit outstanding resolution with a measurable magnitude. To demonstrate the AIC signal transmission, additional applications have been achieved with the exerting of amplitude-shift keying (ASK) signal and frequency-shift keying (FSK) signal. Especially in the frequency modulation (FM) signal transmission mode, the modulated binary baseband signal can be successfully captured, which indicates our devices possess a vast potentiality of ionic informatics.

Results and Discussion

In order to transmit AC signals, two isolated circuits are used for sending and real-time acquiring slight changes of AIC. Two pieces of heavy p-doped silicon are taken as the signal application unit, which would convert the arbitrary voltage signal to the change of electrostatic potential distribution in nanochannels. MXene ($Ti_3C_2T_x$) is chosen as the prototype nanofluidic platform for the information transmission design as it holds great chemical stability and high negative surface charge, which has exhibited extraordinary performance in energy conversion (22–25). The MXene membrane is prepared by a standard vacuum filtration process with a porous polycarbonate membrane, from the dispersion contains liquid exfoliated MXene nanosheets (26). Highly ordered stacked morphology has been further justified with scanning electron microscopy (SEM) images (Fig. 2*B*). The interlaminar space of prepared MXene is only 1.47 nm (Fig. 2*B*), which indicated a vast potentiality of an ideal platform for nanofluidic fabrication. After it is covered with a thin layer of PDMS, the whole nanofluidic device is assembled with PDMS elastomer in a poly(methyl methacrylate) testing container (Fig. 2*A*). Details about the circuitry of source/measure units (SMU) and arbitrarily function generator (AFG) are presented in a corresponding circuit diagram (*SI Appendix*, Fig. S1).

Owing to the flexibility of AFG, almost all kinds of waveforms are accessible for our experiment of alternating ionic transportation. Thus, sine is selected due to its continuous current change and classical pattern for wire and wireless signal transmission. A primary sine function signal can be defined by two variables, frequency (f) and amplitude (A), as shown in Eq. **1**:

$$f(x) = \mathrm{A} \cdot \sin(2\pi fx). \qquad [1]$$

To estimate the possibility of higher information density, both amplitude and frequency need to be adjustable for the process of signal modulation. Thus, five parallel experiments have been conducted at the same nanofluidic device, under sine function stimuli with stepping amplitudes. When the frequency is fixed at 0.5 Hz, the result has shown strong independence between chosen amplitudes and magnitudes of current feedback. As the amplitude increases, the current feedback in the ionic circuit increases symmetrically at both peaks and valleys of time-variant voltage curves, as shown in Fig. 3. When dealing with the current feedback at peaks and valleys, a statistical method was taken due to the unavoidable noise from commercial SMU and slight disturbance in the ionic circuit. The original experimental data require a necessary smoothing process for the following statistical procedure. The adjacent

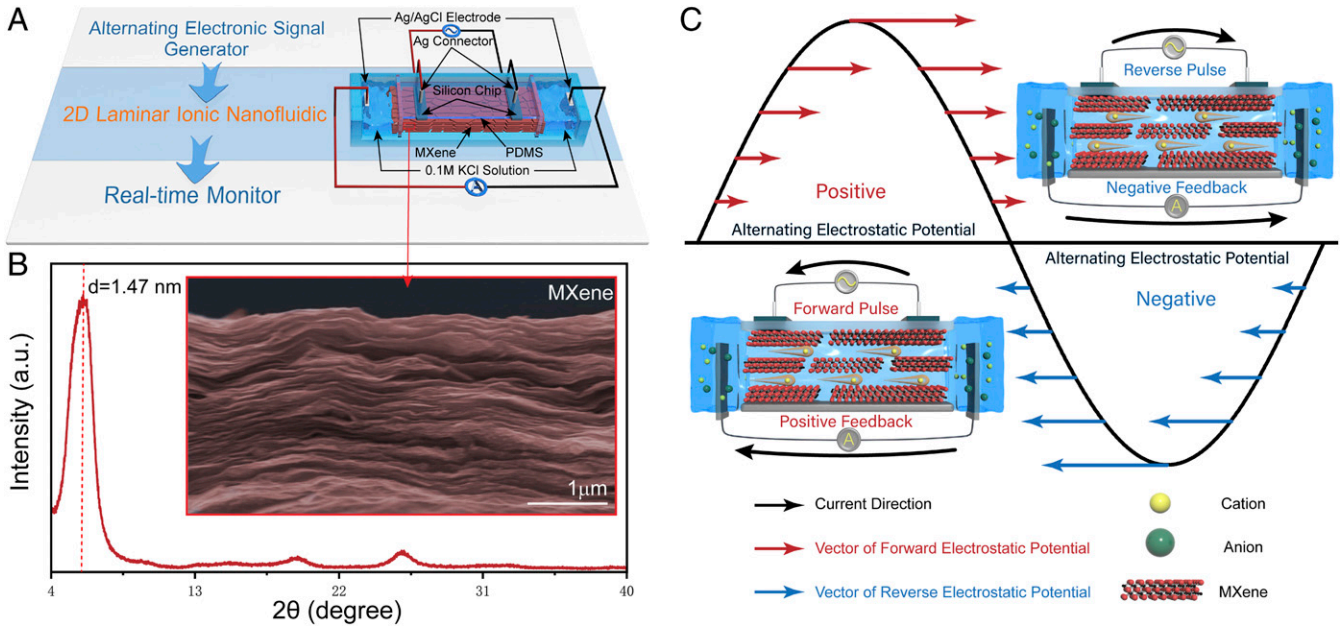

Fig. 2. Device structure and mechanism of AC nanofluidics. (*A*) The alternating ionic nanofluidic devices can be divided into three connected sections; alternating electronic signals are inputted by a commercial arbitrarily/function signal generator, ionic nanofluidic devices for translating the alternating voltage information to the regular forced movement of carriers, and a commercial pico-ammeter to capture the real-time ionic signal in the nanofluidic circuit. (*B*) XRD spectrum and SEM image of the MXene membrane. The interlaminar space is 1.47 nm, converted by Bragg function. (*C*) The mechanism of our alternating ionic nanofluidic devices has been presented. Driven by a sine electrostatic potential (marked with the black curve), AC ionic nanofluidics exhibit two distinctive statuses under forward and reverse pulses. Black arrows demonstrate directions of current. Red and blue arrows represent vectors of electrostatic potential under the corresponding portion of the alternating pulse.

average is chosen because of its lower requirement of the sampling interval compared with the Savitzky–Golay method. Only an isolated peak or valley would be found in half period of smoothed curves, and the numerical loss of smoothed peak value could be well controlled within 5% (*SI Appendix*, Fig. S2). After necessarily smoothing, peaks and valleys in dozens of circles would be analyzed, and further statistics gathered. Gaussian distribution is taken as the fitting method, because of the utterly random noise is the predominant antecedent of indeterminacy. Thus, peak positions of corresponding Gaussian distribution curves are considered as the reasonable value of the current feedback at the same applied electrostatic potential. The peak value analysis for an applied electrostatic potential of 10/−10 V is shown in Fig. 3*B*. All five situations are shown in *SI Appendix*, Fig. S3. The magnitude of current feedback could also be taken as an essential feature for the transmission of the simulated alternating ionic signal. Compared with previous research (27), the microampere feedback is an acceptable magnitude of ionic flux for a 2D laminar nanofluidic with limited thickness. When the driving force is external electrostatic potential with an offset-free sine waveform, the symmetry in magnitudes of AIC feedback extremums is necessary for signal descriptions (Fig. 3*A*). With the increment of applied voltage, the symmetry of AIC feedback dramatically increases, especially when the amplitude is equal to or greater than 4 V. Thus, the determinant of ion transport in a nanochannel can be concluded to be the external electrostatic potential, which imposes physical disturbance on ion transportation in nanochannels (28).

Apart from the controllable ionic current feedback, frequency is another necessary for signal description and transmission. In the sine waveform (Eq. **1**), the adjustable frequency of the sine function is defined by f. Compared with amplitude, frequency demands more consideration, because of its determinant in the informational density of the alternating ionic signal. Herein, a concept from wireless communication is taken to further interpret the importance of frequency in ionic alternating signal transmission. Bandwidth is the difference between the highest and lowest frequencies of a continuous band. In our alternating ionic nanofluidic system, "bandwidth" is a similar parameter, which could describe the range of frequencies for a transmitted alternating signal. Thus, the efficient bandwidth of the transmitted ionic alternating signal is shown in Fig. 4. A series of sine function voltage signals with different frequencies are chosen as the electrostatic potential source in the estimation of an efficient bandwidth. As shown in Fig. 4, captured by Ag/AgCl electrodes, the current feedback in the ionic circuit has a similar sine waveform. The amplitudes at each experimental condition have been normalized for more intuitively counting and demonstrating the quantities of peaks and valleys. At a relatively low output frequency, such as 5 Hz, only one maximum can be founded in a range of 0.1 s. The highest frequency in our experiment is 1,000 Hz, which means 200 extreme points can be found in 0.1 s. The result of statistical processing is 100 peaks and 100 valleys, which indicate a low latency of electric–ionic signal conversion. The result of peaks analysis is shown in Fig. 4. The converted frequency has also been demonstrated with a simple relation:

$$f' = \frac{N}{2 \cdot t}. \qquad [2]$$

f' is the converted frequency, N is the number of extreme points, and t is the time duration of sampling. From the data in Fig. 4, the efficient "bandwidth" is from 5 Hz to 1,000 Hz. The relatively wide bandwidth of the ionic nanofluidic implies a higher information density for more sophisticated signal transmission.

Different from an electric circuit, environmental tolerance is a necessary feature for an ionic nanofluidic circuit (29), which might operate in a more complex aqueous situation. In contrast, this latent defect seems unavoidable in their biological prototype, due to the nature of biological molecules. Owing to the chemical etching process, the aqueous electrochemical nature of 2D laminar materials would give them an extraordinary tolerance

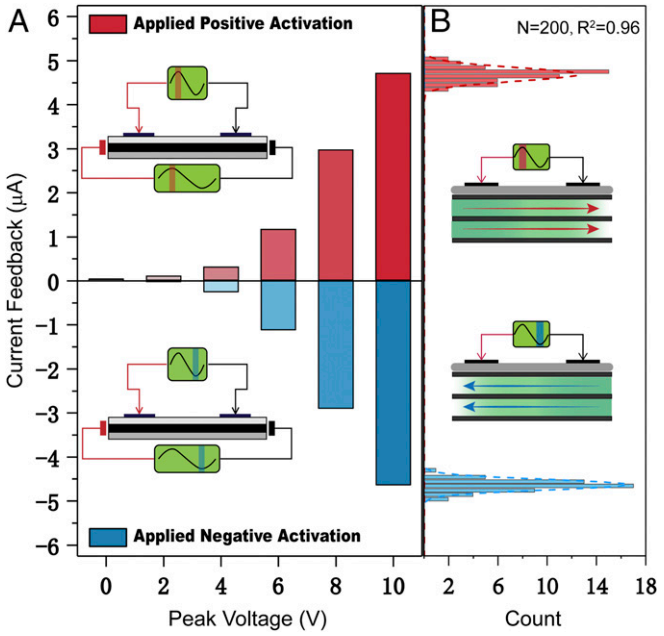

Fig. 3. Ionic current feedback activated with external electrostatic potential. (*A*) The current feedback captured from a 2D laminar nanofluidic device at positive (red) or negative (blue) activating voltages. (*B*) The value of peaks and valleys at ±10 V have been gathered with a statistic data processing. The frequency of peak values has been fitted with a Gaussian distribution with a reasonable determinant coefficient of 0.96. Additional necessary parameters of the Gaussian function are presented in *SI Appendix*, Fig. S3.

in seriously chemical environments, especially extremities of pH conditions. Under different pH values, the undistorted and homologous waveforms of AIC feedbacks indicate the environmental universality for potential application scenarios (*SI Appendix*, Fig. S4). This property is introduced by the serious oxidizing synthesizing procedure (30, 31) of MXene, which can be further verified by the stability of zeta potential. Pure MXene dispersion liquid exhibited ultimately minus zeta potential. Referred to the standpoint of previous studies (32), associated with ionic transport regulation, the different performance of their critical technical indicators is influenced by the functional groups at their exposure sites. This could be also appled to 2D MXene nanofluidics, supported with the features observed in Fourier transform infrared (FTIR) and Raman spectroscopy analysis (*SI Appendix*, Figs. S5 and S6) and elementary information from X-ray photoelectron spectroscopy (*SI Appendix*, Fig. S7).

Based on the flexibility of amplitude, considerable ranges of "transmission bandwidth," and high environmental tolerance, more complex circumstances of ionic signal transmission are possibly accessible. Referring to the development of wireless signal transmission, regular and simple cyclic alternating signal is the elemental stage and fundamental component of ionic informational carriers. One of the most widely applied methods is modulation technology. In the system of amplitude modulation (AM), the amplitude is taken as a variety and would increase or decrease with temporal fluctuations (*SI Appendix*, Fig. S8). The ASK technology, which could modulate a baseband signal in a carrier signal with cyclic changing amplitude, is used to generate a transmitted signal in our ionic nanofluidic. Both concepts of the baseband signal and the carrier signal are borrowed from radio communication technology. In AM signal transmission, as shown in *SI Appendix*, Fig. S8, a sine function with a relatively low frequency (1 Hz) $f(x) = \sin(2\pi x)$ is used as the baseband wave. Baseband wave is the transmitted information. Owing to the universality of sine waveform in radio communication technology, especially the modulation process, another sine function with a relatively high frequency (20 Hz) $f(x) = \sin(40\pi x)$ is used as a carrier wave, on which the baseband signal would be loaded. With the influence of both baseband and carrier signal, the unique current feedback appears in our ionic nanofluidic devices, driven by an AM input. Both responses from the low-frequency baseband

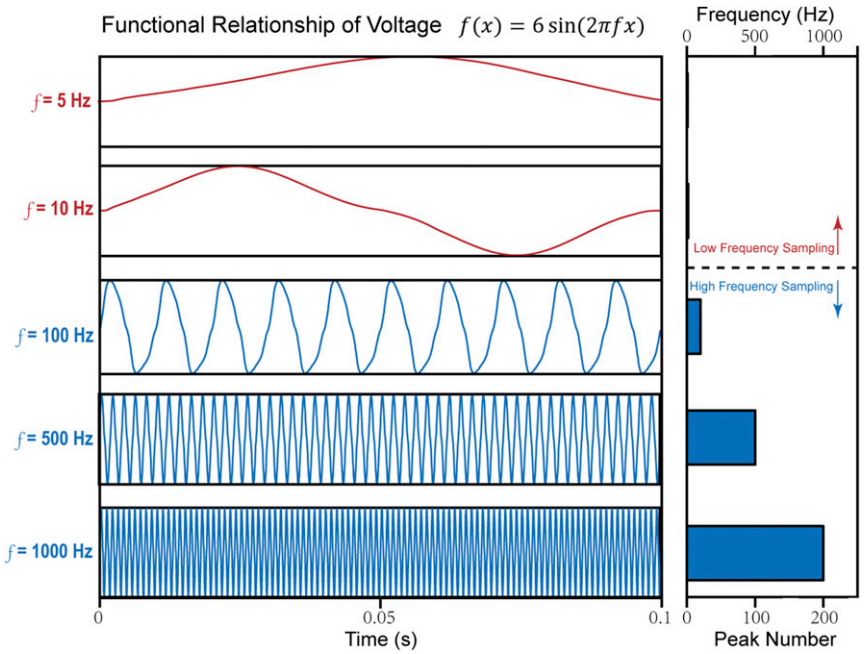

Fig. 4. The efficient bandwidth is through a sine voltage function with variable frequencies. A relatively stable output signal is captured at several individual conditions with different frequencies, 5, 10, 100, 500, and 1,000 Hz. The number of peaks in each diagram of obtained current feedback has been presented with their corresponding converted frequencies. The color marks the corresponding sampling model, where red represents the low-frequency sampling and blue the high-frequency sampling.

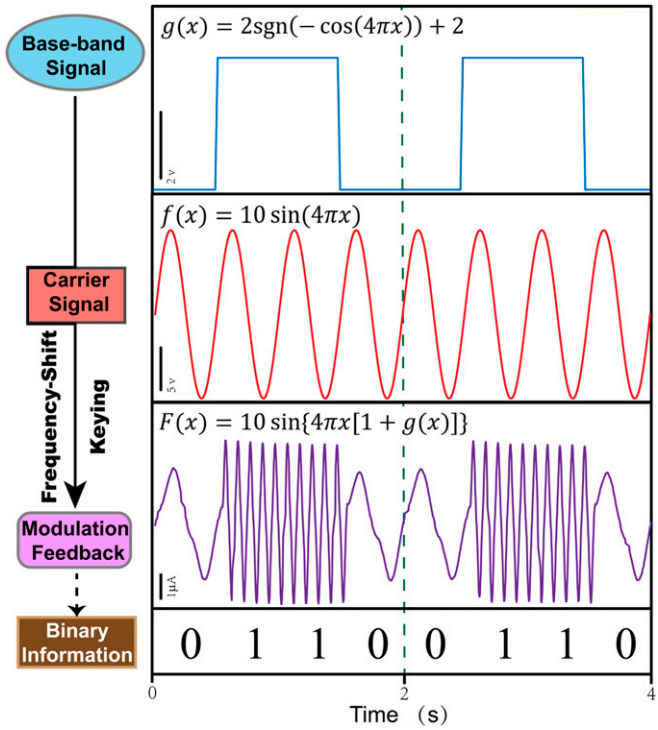

Fig. 5. Frequency-modulated ionic signal transmission. A 1-Hz binary square wave function with offset (blue) is used as the baseband signal $g(x)$. A 2-Hz sine voltage function (red) is used as the carrier signal $f(x)$. The ionic current feedback (purple) triggered by the modulated electric stimulus is also presented. $F(x)$ is the modulating function we used to generate modulated electric stimulus. The binary information, which can be analyzed from the current feedback, is correspondingly listed.

signal and the high-frequency carrier signal can be clearly observed in our current feedback.

Apart from AM technology, FM technology is another nonnegligible section in alternating signal generation. Similar to the amplitude-modulated ionic signal, a frequency-modulated signal has also been transmitted with the help of the most fundamental FSK method. Different from the sine waveform in an AM system, a square wave signal is selected as the baseband signal to achieve binary information transmission (Fig. 5). Its definition and expression have been listed with a frequency of 2 Hz. Here, a square function for FM, $g(x) = 2sgn(-\cos(4\pi x)) + 2$, where $sgn(x)$ could be described with a piecewise function (Eq. **3**),

$$f(x) = \begin{cases} 1, x>0 \\ 0, x = 0 \\ -1, x<0 \end{cases}, \qquad [3]$$

is specially designed with an amplitude of 2 V and an offset of 2 V, which could keep the frequency of modulated signal consistently equal or greater than the frequency of carriers. This destination can be further achieved by the modulating function $F(x) = 10\sin\{4\pi x[1 + g(x)]\}$ and FSK method. After the FSK process, the modulated electrical signal generated by AFG has been applied onto our ionic nanofluidic with the electronic–ionic converter. The ionic current feedback is shown in Fig. 5 with a purple mark. The clarity of the ionic feedback is in a distinguishable range. The frequency of the baseband signal is analytic, due to the observable boundary between different sections. Thus, the binary information in the FSK signal can be further captured. If only high-frequency signals are counted and taken as "open," the information containing alternating "open" and "close" would be discriminated, which is the same as the information distinguished in the transmitted and modulated baseband signal. In a 4-byte information system, this signal can be interpreted as "0110 (binary number)" and "6 (decimal number)." It also indicates the vast potentiality of frequency-modulated and more complex binary signal transmission in our alternating nanofluidic devices.

In conclusion, we have fabricated a bioinspired AC ionic nanofluidic system and an AIC signal generator manipulated by alternating electrostatic potential with a no-contact method. According to the current feedback, an acceptable resolution of the translocated ionic signal can be achieved in a considerable range of amplitudes (from 2 V to 10 V) and frequencies (from 0.5 Hz to 1,000 Hz). This becomes the basis of our signal impulse. Furthermore, in order to testify the possibility of information-carried signal transmission, both FM and AM signals have been applied with the corresponding FSK and ASK method. Both of their characteristic waveforms are successfully reproduced with considerable quality. Especially, a piece of binary information is modulated in the FM signal, which reappears in the ionic circuitry and can be successfully captured and distinguished. Our result demonstrates the biomimetic prototype of constructing ionic circuitry with a 2D laminar nanofluidic system inspired by myelinated sheaths and the feasibility of AIC signal generation and transmission. However, due to the wide compatibility of the mechanism and experimental device, both the form of applied physical filed and the kind of selected 2D materials should not be the limitation of our strategy. We believe that almost all kinds of ionic stimulus–response combinations (33) and directional ionic transportation triggered by physical varieties (34), which has been widely studied, are able to apply on generating alternating ionic signals in 2D laminar nanofluidic systems. Based on the ongoing maturation of ionic nanofluidic technology and the ever-growing reservoir of stimulus–response combinations, it is worthy to push forward one single step from the ionic current manipulation to the new avenue of ionic informatics.

Materials and Methods

Materials preparation, device fabrication, characterization including Raman, X-ray photoelectron spectroscopy, FTIR, X-ray diffraction (XRD) spectrometry, morphologic images of atomic force microscopy, SEM, transmission electron microscopy, selected-area electron diffraction, and additional necessary information is available in *SI Appendix*.

Data Availability. All data associated with this work are available either in the main text or in *SI Appendix*.

ACKNOWLEDGMENTS. We thank Dr. Jinlei Yang for useful support and discussions. This work was supported by the National Key R&D Program of China (Grants 2017YFA0206904 and 2017YFA0206900), National Natural Science Foundation of China (Grants 21625303, 21905287, 51673206, and 21988102), Beijing Natural Science Foundation (Grant 2194088), Strategic Priority Research Program of the Chinese Academy of Sciences (Grant XDA2010213), and the Key Research Program of the Chinese Academy of Sciences (Grant QYZDY-SSW-SLH014).

1. X. Zhang, M. Antonietti, L. Jiang, Bioinformation transformation: From ionics to quantum ionics. *Sci. China Mater.* **63**, 167–171 (2020).
2. L. Wen, X. Zhang, Y. Tian, L. Jiang, Quantum-confined superfluid: From nature to artificial. *Sci. China Mater.* **61**, 1027–1032 (2018).
3. X. Zhang, L. Jiang, Quantum-confined ion superfluid in nerve signal transmission. *Nano Res.* **12**, 1219–1221 (2019).
4. C. Dekker, Solid-state nanopores. *Nat. Nanotechnol.* **2**, 209–215 (2007).
5. Z. Zhang *et al.*, Engineering smart nanofluidic systems for artificial ion channels and ion pumps: From single-pore to multichannel membranes. *Adv. Mater.* **32**, e1904351 (2020).
6. H. Wang, D. D. Kunkel, T. M. Martin, P. A. Schwartzkroin, B. L. Tempel, Heteromultimeric K+ channels in terminal and juxtaparanodal regions of neurons. *Nature* **365**, 75–79 (1993).
7. M. N. Rasband *et al.*, Potassium channel distribution, clustering, and function in remyelinating rat axons. *J. Neurosci.* **18**, 36–47 (1998).

8. X. Shang *et al*., An artificial CO_2-driven ionic gate inspired by olfactory sensory neurons in mosquitoes. *Adv. Mater.* **29**, 1603884 (2017).
9. P. Li *et al*., Light-controlled ion transport through biomimetic DNA-based channels. *Angew. Chem. Int. Ed. Engl.* **55**, 15637–15641 (2016).
10. W. Guan, R. Fan, M. A. Reed, Field-effect reconfigurable nanofluidic ionic diodes. *Nat. Commun.* **2**, 506–513 (2011).
11. R. Karnik *et al*., Electrostatic control of ions and molecules in nanofluidic transistors. *Nano Lett.* **5**, 943–948 (2005).
12. H. Zou *et al*., Alternating current photovoltaic effect. *Adv. Mater.* **32**, 1907249 (2020).
13. A. Brask, D. Snakenborg, J. P. Kutter, H. Bruus, AC electroosmotic pump with bubble-free palladium electrodes and rectifying polymer membrane valves. *Lab Chip* **6**, 280–288 (2006).
14. X. Wu, P. Ramiah Rajasekaran, C. R. Martin, An alternating current electroosmotic pump based on conical nanopore membranes. *ACS Nano* **10**, 4637–4643 (2016).
15. W. Li *et al*., Alternating electric field-induced ion current rectification and electro-osmotic pump in ultranarrow charged carbon nanocones. *Phys. Chem. Chem. Phys.* **20**, 27910–27916 (2018).
16. S. Qin *et al*., Nanofluidic electric generators constructed from boron nitride nanosheet membranes. *Nano Energy* **47**, 368–373 (2018).
17. K. H. Lee *et al*., Ultrasound-driven two-dimensional $Ti_3C_2T_x$ MXene hydrogel generator. *ACS Nano* **14**, 3199–3207 (2020).
18. S. Prakash, A. T. Conlisk, Field effect nanofluidics. *Lab Chip* **16**, 3855–3865 (2016).
19. T. Li *et al*., A nanofluidic ion regulation membrane with aligned cellulose nanofibers. *Sci. Adv.* **4**, eaau4238 (2019).
20. Y. Wang *et al*., Voltage-gated ion transport in two-dimensional sub-1 nm nanofluidic channels. *ACS Nano* **13**, 11793–11799 (2019).
21. M. Fuest, C. Boone, K. K. Rangharajan, A. T. Conlisk, S. Prakash, A three-state nanofluidic field effect switch. *Nano Lett.* **15**, 2365–2371 (2015).
22. P. Liu *et al*., Neutralization reaction assisted chemical-potential-driven ion transport through layered titanium carbides membrane for energy harvesting. *Nano Lett.* **20**, 3593–3601 (2020).
23. L. Ding *et al*., Oppositely charged Ti3C2Tx MXene membranes with 2D nanofluidic channels for osmotic energy harvesting. *Angew. Chem. Int. Ed.* **59**, 8720–8726 (2020).
24. Z. Zhang *et al*., Mechanically strong MXene/Kevlar nanofiber composite membranes as high-performance nanofluidic osmotic power generators. *Nat. Commun.* **10**, 2920 (2019).
25. S. Hong *et al*., Two-dimensional $Ti_3C_2T_x$ MXene membranes as nanofluidic osmotic power generators. *ACS Nano* **13**, 8917–8925 (2019).
26. M. Alhabeb *et al*., Guidelines for synthesis and processing of two-dimensional titanium carbide ($Ti_3C_2T_x$ MXene). *Chem. Mater.* **29**, 7633–7644 (2017).
27. J. Yang, W. Zhu, X. Zhang, F. Chen, L. Jiang, Gated ion transport through layered graphene oxide membranes. *New J. Chem.* **43**, 7190–7193 (2019).
28. S. W. Nam, M. J. Rooks, K. B. Kim, S. M. Rossnagel, Ionic field effect transistors with sub-10 nm multiple nanopores. *Nano Lett.* **9**, 2044–2048 (2009).
29. C. Wang *et al*., Fabrication of stable and flexible nanocomposite membranes comprised of cellulose nanofibers and graphene oxide for nanofluidic ion transport. *ACS Appl. Nano Mater.* **2**, 4193–4202 (2019).
30. M. Hu *et al*., High-capacitance mechanism for $Ti_3C_2T_x$ MXene by in situ electrochemical Raman spectroscopy investigation. *ACS Nano* **10**, 11344–11350 (2016).
31. X. Fan, Y. Ding, Y. Liu, J. Liang, Y. Chen, Plasmonic $Ti_3C_2T_x$ MXene enables highly efficient photothermal conversion for healable and transparent wearable device. *ACS Nano* **13**, 8124–8134 (2019).
32. Z. Zhang *et al*., "Uphill" cation transport: A bioinspired photo-driven ion pump. *Sci. Adv.* **2**, e1600689 (2016).
33. K. Xiao *et al*., Artificial light-driven ion pump for photoelectric energy conversion. *Nat. Commun.* **10**, 74 (2019).
34. J. Yang *et al*., Photo-induced ultrafast active ion transport through graphene oxide membranes. *Nat. Commun.* **10**, 1171 (2019).